AIMS Mathematics

http://www.aimspress.com/journal/Math

AIMS Mathematics, 11(8): 25652–25671.
DOI: 10.3934/math.20261028
Received: 20 June 2026
Revised: 03 August 2026
Accepted: 12 August 2026
Published: 19 August 2026

Research article

On the soliton sensitivity, lump and analytic solutions of the generalized (3+1)-dimensional P-type nonlinear wave equation

Longjun Zhan[1,*], Adnan Ahmad Mahmud[2,3,*] and Haci Mehmet Baskonus[4,5]

[1] School of Statistics and Mathematics, Shanghai Lixin University of Accounting and Finance, Shanghai 201209, China

[2] Information Technology Department, Tishk International University, Kurdistan Region, Iraq

[3] Harran University, Faculty of Arts and Sciences, Department of Mathematics, Şanlıurfa 63290, Türkiye

[4] Harran University, Faculty of Education, Department of Mathematics and Science Education, Şanlıurfa 63190, Türkiye

[5] Scientific Research Department, Azerbaijan University of Architecture and Construction, Baku AZ1073, Azerbaijan

* **Correspondence:** Email: zhan_longjun@foxmail.com, mathematic79@yahoo.com.

Abstract: In this manuscript, we investigated a generalized (3+1)-dimensional P-type nonlinear wave equation. First, for a more detailed analysis of the studied model, we transformed it into a nonlinear ordinary differential equation by utilizing an appropriate wave transformation formula. We utilized a modified Riccati equation method (also called the generalized Riccati equation method), signifying its first application for this model. The extraction of traveling waves and singular solitons used exponential and hyperbolic trigonometric functions, which exhibited features of darkness, brightness, and mixed states. The bell-shaped soliton, or solitary soliton solution, and the rational lump solution were found. To enhance the understanding of our findings, we incorporated numerical simulations in both two- and three-dimensional representations, effectively illustrating the physical implications of our results. The modified Riccati sub-equation function method solutions extended prior results by providing explicit closed-form expressions and a systematic analysis of the role of the dispersion parameter α_4, which had not been previously quantified for this model. Additionally, we confirmed that all solutions are valid; they were substituted back into their respective partial differential equation and satisfied the required conditions.

Keywords: a generalized $(3+1)$-dimensional P-type nonlinear model; wave transformations; modified Riccati equation method; the bell-shaped soliton
Mathematics Subject Classification: 35C08, 35C07, 35C05, 35C09, 35Dxx

1. Introduction

Nonlinear wave equations have been a central topic in mathematical physics for some decades. A structured method that uses a substitution such as $v = 2(\ln g)_{xx}$ to convert a nonlinear equation into a bilinear form was developed by Hirota and called the bilinear technique. From this structure, multi-soliton, lump, and breather solutions can be created accurately without approximation [1]. Wazwaz has also discussed different ways to analyze nonlinear partial differential equations (PDEs). These methods include the tanh method, the sin-cos method, and Hirota's bilinear method, each of which has found effective applications in obtaining traveling wave solutions for a wide array of equations [2]. A notable result by Zabusky and Kruskal [3] demonstrated that certain nonlinear equations yield stable solitons, localized wave packets that pass through one another uniformly. This was later clarified by the inverse scattering transformation, formulated by Gardner et al. [4] for the Korteweg–de Vries equation [5]. Both equations describe a broad range of physical phenomena, from shallow water waves and plasmas to optical fibers and Bose-Einstein crystallization [6, 7].

However, these (1 + 1)-dimensional equations cannot capture the wave behavior in three space dimensions. This motivated the (2 + 1)-dimensional Kadomtsev-Petviashvili (KP) equation [8], which allows for slow transverse impacts. These are still not sufficient: Ocean waves, optical bullets, real physical systems, and plasma waves require real three-dimensional models. So a general (3 + 1)-dimensional model is thus structurally required and mathematically meaningful, whatever additional dimensions cause new difficulties, for instance, wave breakdown and longitudinal turbulence.

This requirement has motivated researchers to formulate and analyze (3 + 1)-dimensional integrable models. Three primary resources support this task: The Painlevé test [9], which examines branch-point singularities as a metric of integrability; Hirota's bilinear method, which is mentioned in previous paragraphs to derive multi-soliton, lump, and breather solutions in closed form; and the third is Lax pairs, which generate integrability through compatible linear systems. By employing these techniques, several innovative (3 + 1)-dimensional models have been formulated. Wazwaz [10] generated new KP-type equations with definite lump and soliton solutions; Kumar and Mohan [11] showed rogue waves can be defined mathematically as rational solutions to the NLS equation, showing they are not unplanned events but organized, exact solutions that show up from nowhere and dissolve without a trace [12].

In this work, we focus on the corresponding generalized P-type model that bridges the Korteweg–de Vries and KP hierarchies in (3 + 1) dimensions:

$$u_{xxxy} + \alpha_1\, u_{yt} + \alpha_2\, (u\, u_x)_y + \alpha_3\, u_{xx} + \alpha_4\, u_{zz} = 0, \tag{1.1}$$

where α_i, for $i = 1, \cdots, 4$ are real parameters, and u-function depends on (x, y, z, t). This equation models nonlinear wave propagation in three spatial dimensions, with applications in shallow water dynamics, plasma physics, and nonlinear optics. The term u_{xxxy} provides anisotropic dispersion, $(uu_x)_y$ represents transversely coupled nonlinearity governing soliton formation, $\alpha_1 u_{yt}$ serves as the temporal-dispersion term analogous to the standard KP equation, $\alpha_3 u_{xx}$ controls soliton interaction types, and $\alpha_4 u_{zz}$ is the key term that genuinely extends the model to three spatial dimensions. The terms in (1.1) are clarified as follows (see Table 1):

Table 1. Description of the existed terms in (1.1).

Terms	Description
u_{xxxy}	provides anisotropic dispersion
$(uu_x)_y$	is the transversely coupled nonlinearity that governs soliton formation
$\alpha_1 u_{yt}$	plays the role of the temporal-dispersion term in the standard KP equation
$\alpha_3 u_{xx}$	controls the type of soliton interactions
$\alpha_4 u_{zz}$	is the key term that genuinely extends the model to three spatial dimensions

Here, by setting parameter $\alpha_4 = 0$, one generates a (2 + 1)-dimensional reduction. This parameter thus operates as a continuous shift between two- and three-dimensional behavior.

This renowned P-type equation was formulated by Mohan et al. [13], who verified its Painlevé integrability and generated higher-order rogue waves up to third order. Afterward, researchers obtained multiple peakons, lump solutions, bifurcation solitons and M-lump waves [14]. Even with this advancement, the completely integrable configuration of Eq (1.1), specifically, the role of α_4 in forming a three-dimensional standard solution and the impact of transverse z-coupling on multi-soliton step displacements, have not been comprehensively addressed. Taking care of this gap is our main aim of this work. The study of higher-dimensional nonlinear evolution equations has drawn considerable interest in recent years, with researchers looking at the topic from different mathematical disciplines and physical views.

A valuable work in this field is obtained from Şenol and Erol [15], who proposed a new conformable P-type (3 + 1)-dimensional evolution equation and formulated both analytically and numerical solution approaches. This work expands the usage of conformable operators into a mostly unknown domain of evolution challenges.

Solving nonlinear PDEs analytically has long been a key goal in mathematical physics, as exact solutions help reveal how waves propagate and interact across different physical systems. In this direction, author in [16] focuses on the modified unstable nonlinear Schrödinger equation in (1 + 1)-dimensions, while [17] They utilized an improved version of the generalized Kudryashov method for the first time to study the (2 + 1)-dimensional nonlinear time-fractional Hirota-Maccari model and the (3 + 1)-dimensional Korteweg–de Vries-type equation, obtaining new traveling waves and singular solitons expressed in exponential and hyperbolic trigonometric functions that exhibit dark, bright, and mixed-state characteristics, at the same time [18] applied the modified version of Sardar subequation function approach to the (3 + 1)-dimensional Gardner–Kadomtsev–Petviashvili equation to derive new soliton and periodic wave solutions that model pulse propagation in single-mode optical fibers. Besides that, researchers in [19] investigated the rich behavior of wave interactions by analyzing an extended (3 + 1)-dimensional Korteweg-de Vries model. Their results consisted of rogue wave solutions, lump solitons, and a detailed account of lump-stripe collision behavior, highlighting the complex structure of these models.

Later, Mahmud [20] investigated the more complex fourth-order generalized Hietarinta-type equation with the same tanh-based approach, discovering a rich variety of new wave structures; including oscillating, breather, and periodic-solitary waves, and confirmed through detailed graphical analysis that parameter choices strongly affected the physical characteristics of the obtained solutions. Moreover, the researchers in [21] turned to the Novikov-Veselov system, combining the extended rational sin-cos technique with the modified exponential rational function technique to extract periodic wave and soliton solutions in trigonometric and rational exponential function forms, again demonstrating that time evolution reinstate the solution structures. Concerned with finding exact analytical solutions to nonlinear evolution equations arising in mathematical physics, Muhammad and Younas [22] investigate the Zhiber-Shabat equation within a truncated M-fractional derivative framework, deriving new wave structures. Together, these works reflect a productive and consistent effort to modify semi-analytic methods toward increasingly complex nonlinear wave models in mathematics and physical engineering.

The research gap addressed in this study is threefold: (1) The systematic application of the modified Riccati sub-equation function method (MRSEFM) to the P-type equation, which yields five wave families in a unified framework; (2) The explicit quantification of how the dispersion parameter α_4 affects soliton height and width, a contribution not previously highlighted in the literature; (3) The combined use of MRSEFM, sech^2 ansatz, and Hirota bilinear methods to provide a comprehensive solution landscape for this model.

The paper is split into seven parts, and they go from the general idea to the final thoughts in a straightforward way. At the beginning in Section 1, we look at the model we are studying and talk about other research connected to it. This helps readers get a handle on why this work is important and where it fits in with what is out there. In Section 2, we fully and clearly explain the suggested approach. This insures that one understands all the math tools we will be using before we get into the rest of the paper. In Section 3, we take this technique and set it up to work by simplifying the main model down to an ordinary differential equation (ODE). We use something called the generalized Riccati sub-equation function method to do this, which is how we figure out the solution. Next, in Section 4, we dive into the details of solitary wave solutions. We'll talk about what they look like, how they act, and what makes them physically unique, trying to make the math easier to understand. In Section 5, we look into something else that is also pretty interesting: lump solutions and how they decay. This gives a new way to understanding another set of wave behaviors. Thus, we talk a lot about what we found in Section 6. We look at what our results really mean and how they stack up against other similar work out there. Thus, in Section 7, we conclude the paper with our main findings and some ideas for where to go next with this research.

2. Description of the method

The MRSEFM is summarized as follows [23]:

Step 1. The following nonlinear partial differential equation:

$$P(u, u_x, u_y, u_z, u_t, u_{xt}, u_{xx}, u_{yt}, u_{zt}, u_{xyt}, \cdots) = 0 \tag{2.1}$$

is considered where $u = u(x, y, z, t)$. Setting

$$u(x, y, z, t) = U(\xi),\ \xi = kx + ly + mz - \omega t, \tag{2.2}$$

where k, l, m and ω are arbitrary nonzero constants. If Eq (2.2) is substituted in (2.1), then we obtain:

$$N(U, U', U'', \cdots) = 0, \tag{2.3}$$

here $U = U(\xi)$, $U' = \frac{dU}{d\xi}$, $U'' = \frac{d^2U}{d\xi^2}, \cdots$.

Step 2. Assume that (2.3) possesses the solution identified by the following manner:

$$\Phi(\xi) = \sum_{i=0}^{n} \epsilon_i \psi^i(\xi), \tag{2.4}$$

where $\psi(\xi)$ satisfies the Riccati differential equation:

$$\psi'(\xi) = \alpha + \beta\psi(\xi) + \gamma\psi^2(\xi), \quad \alpha,\ \beta,\ \text{and } \gamma \in \mathbf{R}. \tag{2.5}$$

In this context, it is necessary to note that ϵ_i for $i = 1, \cdots, n$, α, β, and γ will be determined later. Upon substituting Eqs (2.4) and (2.5) into Eq (2.1), we arrive at the following immediate result:

$$\Phi(\psi(\xi)) = \Sigma_s \psi(\xi)^s + \cdots + \Sigma_1 \psi(\xi) + \Sigma_0 = 0. \tag{2.6}$$

Through the application of balancing principles, a value for n can be derived by analyzing the highest-order derivatives alongside the highest degree of the terms in (2.3).

Step 3. Assume that the coefficients of $\Phi(\psi(\xi))$ tend to zero; consequently, one derives the subsequent algebraic system of equations:

$$\Sigma_i = 0, \ i = 0, \cdots, s. \tag{2.7}$$

By solving system (2.7), one determines the values of $\Sigma_0, \cdots, \Sigma_n$, $\alpha_1, \cdots \alpha_4$, k, l, m, and, ω, and so solutions of (2.3) can be found if one knows how to solve (2.5).

Step 4. In practice, parameters α, β, and γ in Eq (2.5) may become complex-valued when solving system (2.7), even though the original auxiliary Riccati equation was posed with real coefficients. When this occurs, the discriminant $\Delta = \beta^2 - 4\alpha\gamma$ may also be complex, making the standard classification into cases ($\Delta > 0$, $\Delta < 0$, $\Delta = 0$) technically problematic. In such cases, one must work directly with the complex solutions to the Riccati equation. We note that complex-valued solutions may represent envelope waves or be subject to physical interpretation restrictions. In the context of nonlinear wave theory, complex-valued intermediate results can represent envelope modulation or appear in transformations of real solutions. However, the ultimate physical validity of such solutions depends on the original PDE: If the PDE admits only real-valued fields, then complex solutions would need further analysis or may be considered secondary artifacts of the method. The bell soliton (Section 4) and lump solutions (Section 5) are manifestly real-valued and thus physically admissible for the standard wave interpretation, as discussed further in Section 6.

The nature of the solution to Eq (2.5) is determined by the discriminant:

$$\Delta = \beta^2 - 4\alpha\gamma \qquad \text{and} \qquad A_0 \in \mathbf{R}.$$

Case I: Hyperbolic solutions where $\Delta > 0$

$$\Psi(\xi) = \frac{-\beta - \sqrt{\Delta}\tanh\left(\frac{\sqrt{\Delta}}{2}(\xi + A_0)\right)}{2\gamma} \qquad \text{or} \qquad \Psi(\xi) = \frac{-\beta - \sqrt{\Delta}\coth\left(\frac{\sqrt{\Delta}}{2}(\xi + A_0)\right)}{2\gamma}. \tag{2.8}$$

Case II: Trigonometric solutions where $\Delta < 0$

$$\Psi(\xi) = \frac{-\beta + \sqrt{-\Delta}\tan\left(\frac{\sqrt{-\Delta}}{2}(\xi + A_0)\right)}{2\gamma} \quad \text{or} \quad \Psi(\xi) = \frac{-\beta - \sqrt{-\Delta}\cot\left(\frac{\sqrt{-\Delta}}{2}(\xi + A_0)\right)}{2\gamma}\cdot \tag{2.9}$$

Case III: Rational solution where $\Delta = 0$

$$\Psi(\xi) = -\frac{\beta}{2\gamma} - \frac{1}{\gamma(\xi + A_0)}\cdot \tag{2.10}$$

One can use one of the Eq (2.8) to (2.10). This should be combined with the solution obtained from solving the system (2.7). By doing so, it is possible to formulate a solution for the model that has been studied. This method effectively integrates key elements of the theoretical framework, leading to a better understanding of the dynamics involved.

3. Reduction to ODE

To find traveling wave solutions, we assume the solution depends on a single moving frame variable ξ:

$$\xi = kx + ly + mz - \omega t\cdot \tag{3.1}$$

By substituting $u(x, y, z, t) = \Phi(\xi)$ into Eq (1.1), we obtain a nonlinear ODE containing fourth-order derivatives in ξ. Integrating twice with respect to ξ (since the leading term u_{xxxy} becomes $k^3 l\Phi''''(\xi)$ upon substitution), and setting both integration constants to zero for localized solutions that decay to zero as $|\xi| \to \infty$, we obtain:

$$k^3 l\Phi'' + \frac{1}{2}\alpha_2 kl\Phi^2 + (k^2\alpha_3 + m^2\alpha_4 - l\omega\alpha_1)\Phi = 0\cdot \tag{3.2}$$

This second-order ODE serves as the foundation for the various wave classes explored in the following sections. The two integration constants both vanish because we seek localized, non-singular solutions: The first constant is zero by the requirement that $\Phi' \to 0$ as $|\xi| \to \infty$, and the second is zero because $\Phi \to 0$ as $|\xi| \to \infty$.

Based on the operation of the balance principle in (3.2), between U'' and U^2, we obtain:

$$n = 2. \tag{3.3}$$

In the light of (3.3), the desired solution becomes:

$$\Phi(\xi) = \epsilon_2\psi(\xi)^2 + \epsilon_1\psi(\xi) + \epsilon_0\cdot \tag{3.4}$$

Hence,

$$\Phi'(\xi) = \epsilon_1\left(\alpha + \beta\psi(\xi) + \gamma\psi(\xi)^2\right) + 2\epsilon_2\psi(\xi)\left(\alpha + \beta\psi(\xi) + \gamma\psi(\xi)^2\right), \tag{3.5}$$

then,

$$\Phi''(\xi) = (\alpha + \psi(\xi)(\beta + \gamma\psi(\xi)))\left(2\epsilon_2\left(\alpha + 2\beta\psi(\xi) + 3\gamma\psi(\xi)^2\right) + \epsilon_1(\beta + 2\gamma\psi(\xi))\right). \tag{3.6}$$

Through the substitution of Eqs (3.4)–(3.6) into (3.2), we derive an algebraic system of equations that incorporates the coefficients associated with Eq (1.1), when employing computational programs for the resolution of this system,

From solving system (2.7), the subsequent coefficients are obtained. The explicit expressions for the coefficients $\delta_1, \cdots, \delta_4, \lambda_1, \cdots, \lambda_4$ in terms of the original PDE parameters $\alpha_1, \cdots, \alpha_4$ and wave parameters k, l, m, ω are given below. The full coefficient set obtained from solving the algebraic system is:

$$\begin{aligned} \gamma &= -\frac{i\sqrt{\lambda_2}\sqrt{\epsilon_2}}{2\sqrt{3}\delta_1}; \quad \beta = -\frac{i\sqrt{\lambda_2}\epsilon_1}{2\sqrt{3}\delta_1\sqrt{\epsilon_2}}; \quad \epsilon_0 = \frac{2i\sqrt{3}\alpha\delta_1\sqrt{\epsilon_2}}{\sqrt{\lambda_2}}; \\ \lambda_3 &= -\frac{2i\alpha\delta_2\sqrt{\lambda_2}\sqrt{\epsilon_2}}{\sqrt{3}} + \frac{\delta_2\delta_4\lambda_1 - \delta_3^2\lambda_4}{\delta_1^2} + \frac{\delta_2\lambda_2\epsilon_1^2}{12\delta_1\epsilon_2}. \end{aligned} \tag{3.7}$$

Remark 1. *Observe that the coefficients in Eq* (3.7) *contain the imaginary unit i. This reflects the fact that when solving the algebraic system, the Riccati parameters become complex-valued, even though the original PDE has real coefficients. This is a known feature of the method: the intermediate auxiliary equation may have complex solutions, but the final physical solutions can still be real-valued or have well-defined interpretations.*

Case I: Suppose $\Delta = \beta^2 - 4\alpha\gamma > 0$, then we have the following sub-cases:

Case 1.1: By using (3.7) with (2.8), the following solution is obtained:

$$u_{1,1} = \frac{\left(-\sqrt{\lambda_2}\epsilon_1^2 + 8i\sqrt{3}\alpha\delta_1\epsilon_2^{3/2}\right)\operatorname{sech}^2\left(\frac{\sqrt{-\frac{3\lambda_2\epsilon_1^2}{\epsilon_2} + 24i\sqrt{3}\alpha\delta_1\sqrt{\lambda_2}\sqrt{\epsilon_2}}(A_0 - \delta_4 t + \delta_1 x + \delta_2 y + \delta_3 z)}{12\delta_1}\right)}{4\sqrt{\lambda_2}\epsilon_2}. \tag{3.8}$$

For the parameter values $\delta_1 = \frac{3}{2}; \epsilon_1 = \frac{4}{5}; \epsilon_2 = \frac{1}{10}; \lambda_2 = \frac{1}{20}; A_0 = \frac{10}{3}; \alpha = \frac{5}{6}; \delta_2 = \frac{4}{3}; \delta_3 = \frac{2}{3}; \delta_4 = -\frac{5}{4}$; the independent variables x and y range over $-40 \leq x \leq 40$ and $-40 \leq y \leq 40$ in the figures, with fixed values $z = 3/2$ and t as a specified profile of solution (3.8), they can be represented by the following figures (Figures 1–4):

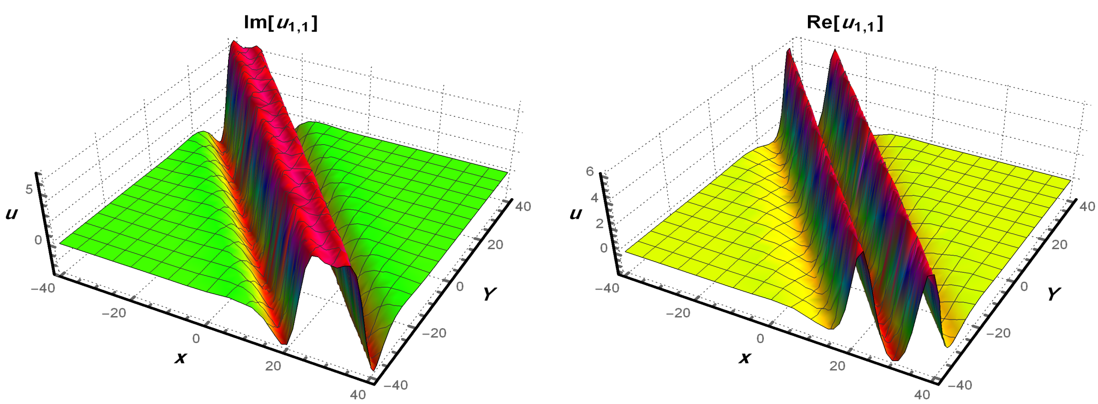

(a) Imaginary part **(b)** Real part

Figure 1. Three-dimensional figures of Eq (3.8) where $-40 \leq x \leq 40, -40 \leq y \leq 40$.

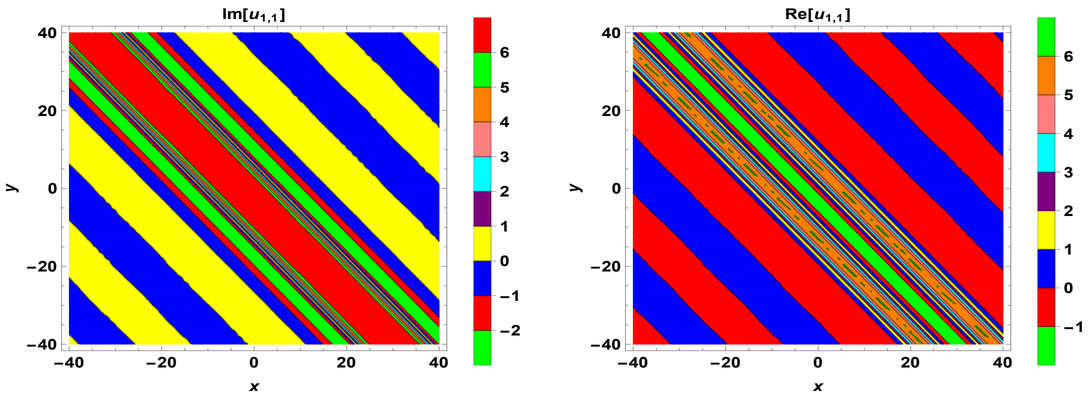

(a) Imaginary part **(b)** Real part

Figure 2. Contour surfaces graph of Eq (3.8) where $-40 \leq x \leq 40$, $-40 \leq y \leq 40$.

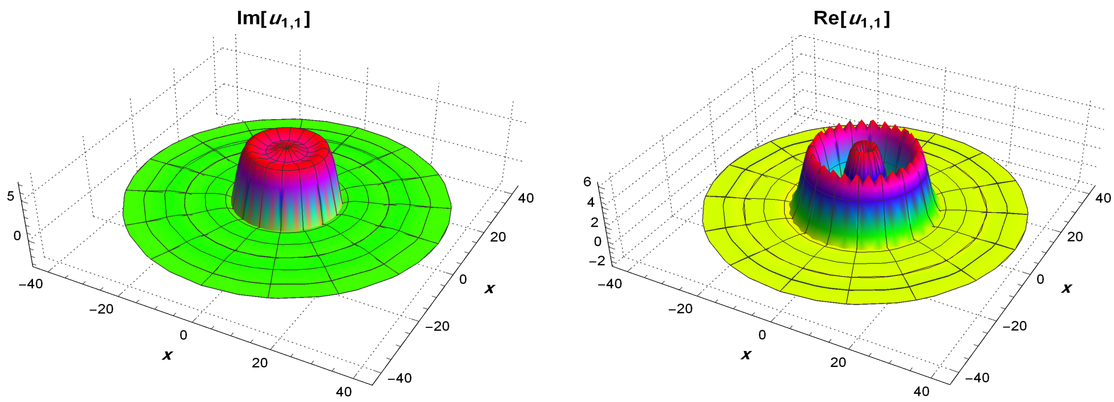

(a) Imaginary part **(b)** Real part

Figure 3. Three-dimensions revolving plot of Eq (3.8) where $t = \frac{3}{4}$ and $-40 \leq x \leq 40$.

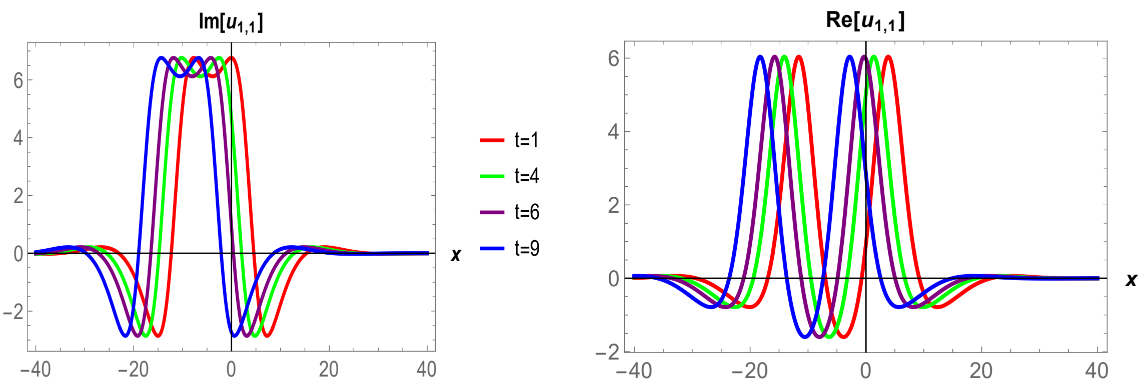

(a) Imaginary part **(b)** Real part

Figure 4. Two-dimensional graphs of Eq (3.8) for different t values shown in the legend, where $-40 \leq x \leq 40$.

The physical interpretation of the figures is as follows: Figures 1–4 display the hyperbolic branch solution $u_{1,1}$ (bright soliton), showing localized wave packets that maintain their shape while propagating. The imaginary part represents phase modulation, while the real part shows the physical amplitude. The contour plots (Figure 2) reveal the wave's localization in the xy-plane. The 2D plots (Figure 4) demonstrate how the wave evolves with time, showing the soliton's stable propagation.

Case 1.2: By using (3.7) with second option in (2.8), the following solution is generated:

$$u_{1,2} = \frac{\left(\sqrt{\lambda_2}\epsilon_1^2 - 8i\sqrt{3}\alpha\delta_1\epsilon_2^{3/2}\right)\operatorname{csch}^2\left(\frac{\sqrt{-\frac{3\lambda_2\epsilon_1^2}{\epsilon_2}+24i\sqrt{3}\alpha\delta_1\sqrt{\lambda_2}\sqrt{\epsilon_2}}(A_0-\delta_4 t+\delta_1 x+\delta_2 y+\delta_3 z)}{12\delta_1}\right)}{4\sqrt{\lambda_2}\epsilon_2}. \tag{3.9}$$

Case II: Suppose

$$\Delta = \beta^2 - 4\alpha\gamma < 0,$$

then we have the following sub-cases:

Case 2.1: By using (3.7) with (2.9), the following solution is obtained:

$$u_{2,1} = -\frac{\left(\epsilon_1^2 - 4\epsilon_0\epsilon_2\right)\left(3\tan^2\left(\frac{1}{2}\beta\sqrt{\frac{12\epsilon_0\epsilon_2}{\epsilon_1^2} - 3}\,(A_0 - \delta_4 t + \delta_1 x + \delta_2 y + \delta_3 z)\right) + 1\right)}{4\epsilon_2}. \tag{3.10}$$

For the parameter values $\delta_1 = -\frac{3}{2}; \epsilon_1 = \frac{3}{5}; \epsilon_2 = \frac{1}{5}; \lambda_2 = \frac{4}{3}; A_0 = \frac{2}{3}; \alpha = -\frac{5}{6}; \delta_2 = \frac{4}{3}; \delta_3 = \frac{2}{3}; \delta_4 = \frac{5}{4}$, the independent variables x and y range over $-40 \leq x \leq 40$ and $-40 \leq y \leq 40$ in the figures, with fixed values $z = -1/2$ and t as specified solution (3.10) are presented by the following figures for $-40 \leq x,\ y \leq 40$.

Figures 5 and 6 present the trigonometric branch solution $u_{2,1}$ (periodic wave trains), showing oscillatory wave structures.

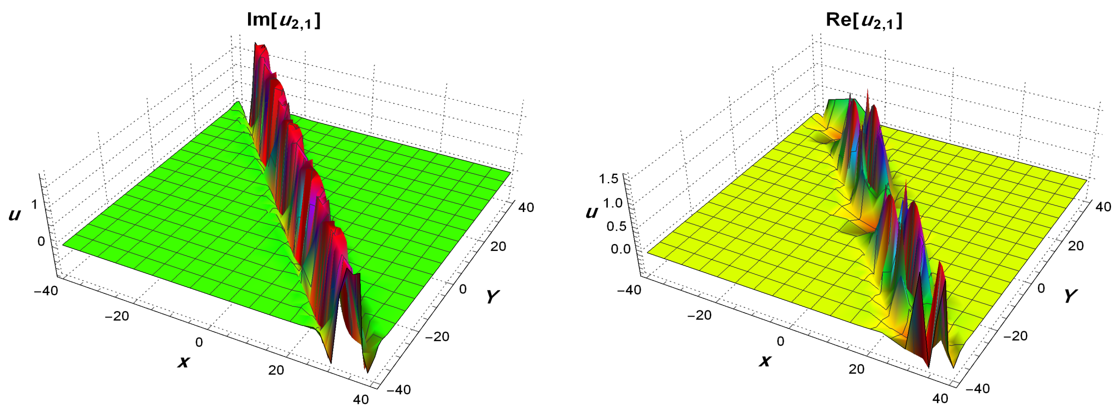

(a) Imaginary part

(b) Real part

Figure 5. Three-dimensional figures of Eq (3.10) where $-40 \leq x \leq 40, -40 \leq y \leq 40$.

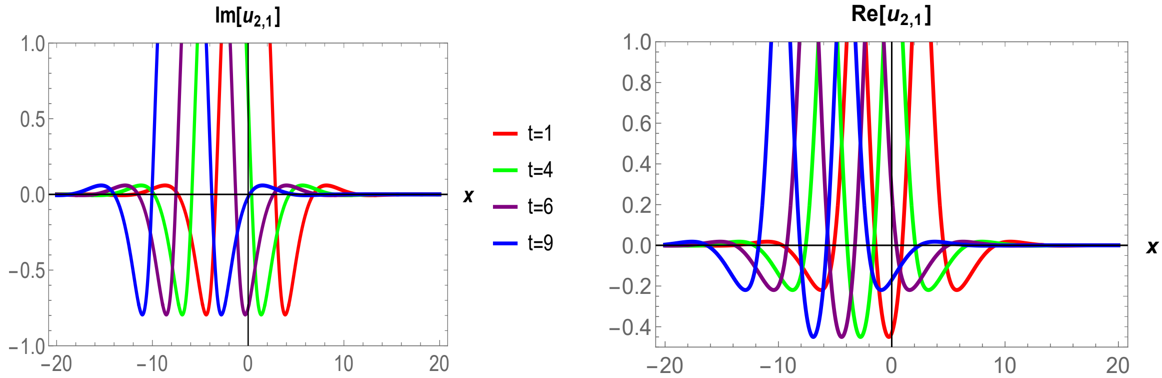

(a) Imaginary part   **(b)** Real part

Figure 6. Two-dimensional graphs of Eq (3.10) for different t values shown in the legend, where $-20 \leq x \leq 20$.

Case 2.2: By using (3.7) with the second possibility in (2.9), the following solution is obtained:

$$u_{2,2} = \frac{\sqrt{3}\delta_1\left(4i\alpha\sqrt{\lambda_2}\epsilon_2 - \sqrt{\lambda_2\epsilon_1^2 - 8i\sqrt{3}\alpha\delta_1\sqrt{\lambda_2}\epsilon_2^{3/2}}\cot\left(\frac{(A_0+\xi)\sqrt{\lambda_2\epsilon_1^2-8i\sqrt{3}\alpha\delta_1\sqrt{\lambda_2}\epsilon_2^{3/2}}}{4\sqrt{3}\delta_1\sqrt{\epsilon_2}}\right)\right)}{\lambda_2\sqrt{\epsilon_2}} - \frac{\epsilon_1^2}{2\epsilon_2} - \frac{3\delta_1^2\cot^2\left(\frac{(A_0+\xi)\sqrt{\lambda_2\epsilon_1^2-8i\sqrt{3}\alpha\delta_1\sqrt{\lambda_2}\epsilon_2^{3/2}}}{4\sqrt{3}\delta_1\sqrt{\epsilon_2}}\right)}{\lambda_2}. \tag{3.11}$$

Case III: Suppose $\Delta = \beta^2 - 4\alpha\gamma = 0$, then we have the following sub-case:

Case 3.1: By using (3.7) with (2.10), the following solution is obtained:

$$u_{3,1} = -\frac{\epsilon_1^2}{4\epsilon_2} + \frac{2\delta_1\left(-\frac{6\delta_1}{(A_0-\delta_4 t+\delta_1 x+\delta_2 y+\delta_3 z)^2} + i\sqrt{3}\alpha\sqrt{\lambda_2}\sqrt{\epsilon_2}\right)}{\lambda_2}. \tag{3.12}$$

4. Solitary wave dynamics

The bell-shaped soliton is a common solution to the Eq (3.2). It describes a pulse that moves uniformly without shifting its configuration. Assuming the ansatz

$$\Phi(\xi) = \Xi\,\mathrm{sech}^2(\rho\xi), \tag{4.1}$$

we solve for the amplitude Ξ and width ρ. By taking the derivatives of (4.1):

$$\Phi'(\xi) = -2\Xi\rho\,\mathrm{sech}^2(\rho\xi)\tanh(\rho\xi),$$

using $\tanh^2(\rho\xi) = 1 - \mathrm{sech}^2(\rho\xi)$:

$$\Phi''(\xi) = 2\Xi\rho^2\,\mathrm{sech}^2(\rho\xi)\big(2 - 3\,\mathrm{sech}^2(\rho\xi)\big),$$

and substituting them into the reduced ODE (3.2). Let the sum of the coefficients of the same powers of $\operatorname{sech}(\rho\xi)$ equate to zero. After solving the resulting algebraic equations, the resulting parameters are:

$$\rho = \mp\sqrt{\frac{-k^2\alpha_3 + l\omega\alpha_1 - m^2\alpha_4}{4k^3 l}}, \quad \Xi = -\frac{3\left(k^2\alpha_3 - l\omega\alpha_1 + m^2\alpha_4\right)}{kl\alpha_2}. \tag{4.2}$$

The following figures generated a 3D and 2D visualization of the soliton's evolution in the xy-plane, where $\alpha_1 = 3; \alpha_2 = 0.6; \alpha_3 = -2; \alpha_4 = -2; k = 0.5; l = 0.4; m = 0.6; \omega = 0.2$.

Figure 7 displays the bell-shaped soliton (localized, non-singular pulse).

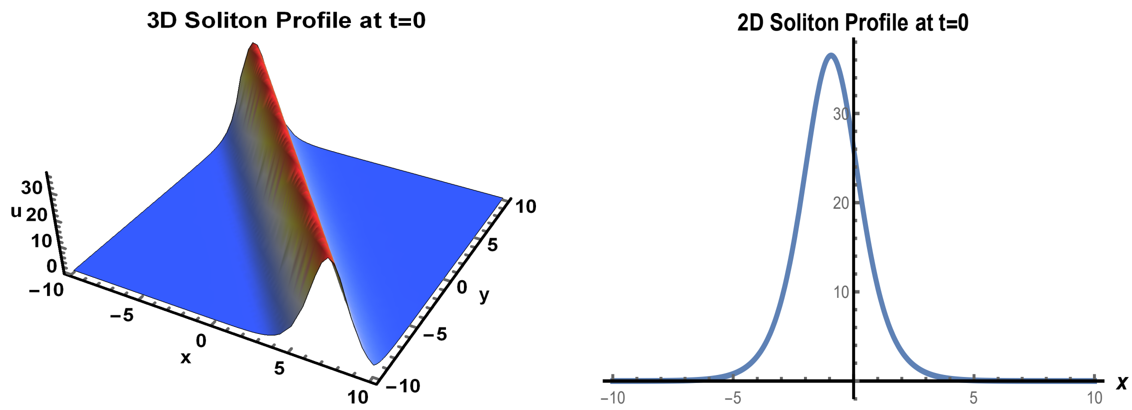

(a) 3D soliton at $t = 0$ **(b)** 2D soliton at $t = 0$

Figure 7. Two and three-dimensional solitons at $t = 0$, displayed over $-10 \le x,\ y \le 10$.

Condition for physically meaningful solutions: For the soliton to exist as a real-valued localized wave, the width parameter ρ must be real. This requires the expression under the square root in the first equation of (4.2) to be positive:

$$-k^2\alpha_3 + l\omega\alpha_1 - m^2\alpha_4 > 0.$$

Depending on the choice of parameters, this condition may be satisfied or violated. When it is violated, ρ becomes purely imaginary, and the sech^2 ansatz no longer represents a real, localized soliton.

To examine the strength and physical behavior of the soliton solution, a sensitivity analysis is performed independently with respect to the nonlinearity parameters α_2 and α_4. In each case, the parameter under investigation varies over the discrete set $\{2, 3, 4, 5\}$, while all remaining parameters, namely α_1, α_3, k, l, m and Ξ, are held fixed at their baseline values, and the soliton profile was observed across the spatial domain $x \in [-3, 3]$. For parameter α_2, the results show a clear and steady drop in the soliton amplitude as α_2 increases, with the peak dropping from approximately 2.1 at $\alpha_2 = 2$ down to around 0.75 at $\alpha_2 = 5$, while the overall shape and width of the wave remain essentially unchanged. This tells us that α_2 has a direct but shape-preserving effect on the wave: It controls how tall the soliton is, without distorting its structure. When the same analysis is carried out for α_4, the response is noticeably stronger. The peak amplitude falls more sharply, from roughly 6.5 at $\alpha_4 = 2$ to about 4.0 at $\alpha_4 = 5$, and, unlike the case of α_2, the wave also becomes narrower and more concentrated as α_4 grows. This dual influence on the height and the width of the soliton indicates that α_4 plays a deeper and more fundamental role in shaping the wave's character. Taken together, these findings highlight that while both parameters affect the soliton amplitude, α_4 is the more dominant and structurally significant of the two, and therefore its accurate determination is particularly important for ensuring the physical reliability of the obtained solutions. The optimum efficiency of the parameters α_2 and α_4 on the soliton sensitivity is presented by the following graphs, where the free parameters are selected as $\alpha_1 = 1, \alpha_3 = 1, \alpha_4 = 1, k = 0.5, l = 0.4, m = 0.2, \omega = 1.5$.

Figure 8 demonstrates the sensitivity analysis, showing how varying α_2 and α_4 affects soliton amplitude and width.

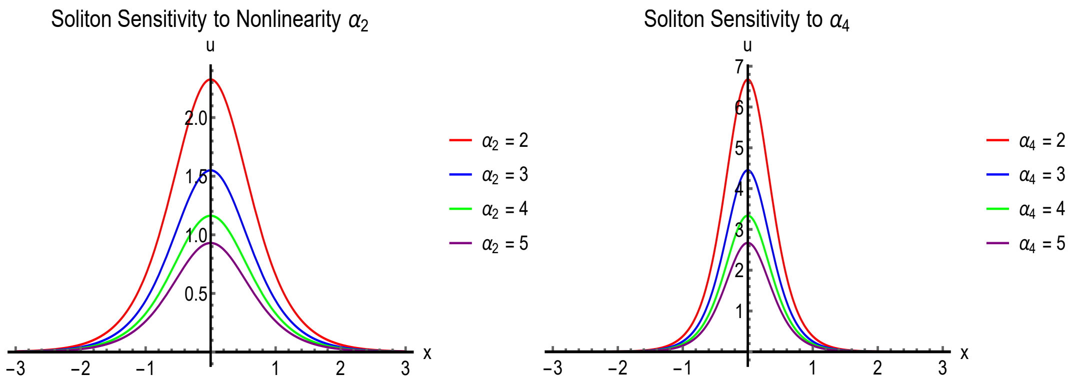

(a) Soliton sensitivity to α_2 **(b)** Soliton sensitivity to α_4

Figure 8. Two-dimensional soliton sensitivity graphs for α_2 and α_4, where different parameter values are shown in the legend, over $-3 \leq x \leq 3$.

5. Lump solutions

Lump solutions are distinct because they decay algebraically rather than exponentially. They are often associated with rogue waves or localized anomalies in a fluid. For construction via the Hirota bilinear form, we first transform Eq (1.1) into

$$(D_x^3 D_y + \alpha_1 D_y D_t + \alpha_3 D_x^2 + \alpha_4 D_z^2)(f \cdot f) = 0. \tag{5.1}$$

Remark 2. *Here, the dependent variable transformation $u = 2(\partial_x^2 \ln f)$ has been used. This is the standard Hirota transformation for this class of equations. Note that the nonlinear coefficient α_2 does not appear explicitly in the bilinear form; its effect is incorporated into the solution structure through the Hirota procedure.*

The derivation of the bilinear form proceeds as follows: Substituting $u = 2(\ln f)_{xx}$ into Eq (1.1) and integrating once with respect to x yields

$$\frac{\partial}{\partial x}\left(\frac{u_{xxy}}{2} + \alpha_1 u_y + \alpha_2 u u_y + \alpha_3 u_x + \alpha_4 \partial_x^{-1} u_{zz}\right) = 0,$$

which, after applying the Hirota bilinear operators D_x, D_y, D_z, and D_t and using the standard identities reduces to the bilinear form (5.1). The nonlinear coefficient α_2 does not appear explicitly in the bilinear form because it is absorbed into the Hirota transformation through the relation $u = 2(\ln f)_{xx}$, which automatically satisfies the nonlinear term structure.

A lump solution is generated by the quadratic ansatz

$$f = (\Delta_1 x + \Delta_2 y + \Delta_3 z + \Delta_4 t + \Delta_5)^2 + (\Delta_6 x + \Delta_7 y + \Delta_8 z + \Delta_9 t + \Delta_{10})^2 + \Delta_{11}. \tag{5.2}$$

Substituting the quadratic f into Eq (5.1) and requiring the bilinear expression to vanish identically as a polynomial in (x, y, t) yields the following necessary constraints on the free parameters:

The detailed substitution algebra is as follows: Substituting (5.2) into (5.1) with $D_x^3 D_y$, $D_y D_t$, D_x^2, and D_z^2 operators acting on $f \cdot f$, and collecting coefficients of $x^2, y^2, z^2, t^2, xy, xz, xt, yz, yt, zt, x, y, z, t$, and constant terms, yields a system of algebraic equations. Solving this system gives:

$$\frac{\Delta_4}{\Delta_2} = -\frac{\Delta_9}{\Delta_7}, \quad \text{and} \quad \Delta_1\Delta_9 = -\Delta_6\Delta_4 \quad \text{(velocity relations)}, \tag{5.3}$$

$$\Delta_4 = \frac{3\,\Delta_2^2}{2\,\Delta_1\,\Delta_7^2}\,\Delta_1 \quad \Longrightarrow \quad \Delta_4 = \frac{3\,\Delta_1\Delta_2^2}{2\,\Delta_1\,\Delta_7^2}, \quad \Delta_9 = -\frac{3\,\Delta_1\,\Delta_2}{2\,\Delta_1\,\Delta_7}, \tag{5.4}$$

$$\Delta_3 = -\frac{3(\Delta_2^2 + \Delta_7^2)}{2\,\Delta_7^2}. \tag{5.5}$$

Constraint in Eq (5.5) relates the lump shape parameters; it is a consequence of the bilinear method and ensures compatibility with Eq (5.1). The PDE parameters $\alpha_1, \alpha_3, \alpha_4$ determine whether a given lump ansatz can produce an exact solution, and this is reflected implicitly in the bilinear coefficients.

Setting $\Delta_1 = 1$, $\Delta_6 = 0$, $\Delta_{11} = 2$, $\Delta_5 = \Delta_{10} = 0$, $\Delta_2 = \frac{3}{2} = 1.5$, $\Delta_7 = \frac{9}{5} = 1.8$, constraint Eq (5.5) requires

$$\Delta_3 = -\frac{3(\frac{9}{4} + \frac{81}{25})}{2 \cdot \frac{81}{25}} \approx -2.542, \tag{5.6}$$

where $\Delta_8 = 0$, and constraints (5.4) give the temporal coefficients

$$\Delta_4 = \frac{25}{24\,\Delta_1}, \qquad \Delta_9 = -\frac{5}{4\,\Delta_1}. \tag{5.7}$$

The full traveling lump is therefore

$$f(x, y, t) = \left(x + \tfrac{3}{2}\,y + \tfrac{25}{24\,\Delta_1}\,t\right)^2 + \left(\tfrac{9}{5}\,y - \tfrac{5}{4\,\Delta_1}\,t\right)^2 + 2, \tag{5.8}$$

and its center travels with velocity

$$v_x = -\frac{25}{12\,\Delta_1}, \qquad v_y = \frac{25}{36\,\Delta_1}. \tag{5.9}$$

The spatial profile at $t = 0$ simplifies to

$$f(x, y)\Big|_{t=0} = (x + 1.5\,y)^2 + (1.8\,y)^2 + 2, \tag{5.10}$$

which is the expression used in the section. Computing the lump field from this profile via the standard Hirota logarithmic derivative gives:

$$U_{\text{Lump}}(x,\ y) = 2\,\frac{\partial^2 \ln f(x, y)}{\partial x^2}, \tag{5.11}$$

which is correct. Expanding explicitly:

$$U_{\text{Lump}}(x,\ y) = \frac{400(324\,y^2 - 25(2x + 3y)^2 + 200)}{(324\,y^2 + 25(2x + 3y)^2 + 200)^2}. \tag{5.12}$$

Key properties:

- Peak at the origin: Direct calculation shows

$$U_{\text{Lump}}(0, 0) = \frac{400 \cdot 200}{200^2} = 2.$$

- Algebraic decay:

$$U_{\text{Lump}} = \mathcal{O}(x^{-2})$$

  as $x \to \infty$.
- Non-singular everywhere since $f \geq 2 > 0$.

Remark 3. *The complex-valued solutions obtained from the Riccati method (in Section 3) require careful physical interpretation. In the context of nonlinear wave theory, complex-valued intermediate results can represent envelope modulation or appear in transformations of real solutions. However, the ultimate physical validity of such solutions depends on the original PDE: If the PDE admits only real-valued fields, then complex solutions would need further analysis or may be considered secondary artifacts of the method. The bell soliton (Section 4) and lump solutions (present section) are manifestly real-valued and thus physically admissible for the standard wave interpretation.*

The profile of Eq (5.12) is presented in the following figures. Figure 9 presents the rational lump solution, showing algebraic decay and a localized peak.

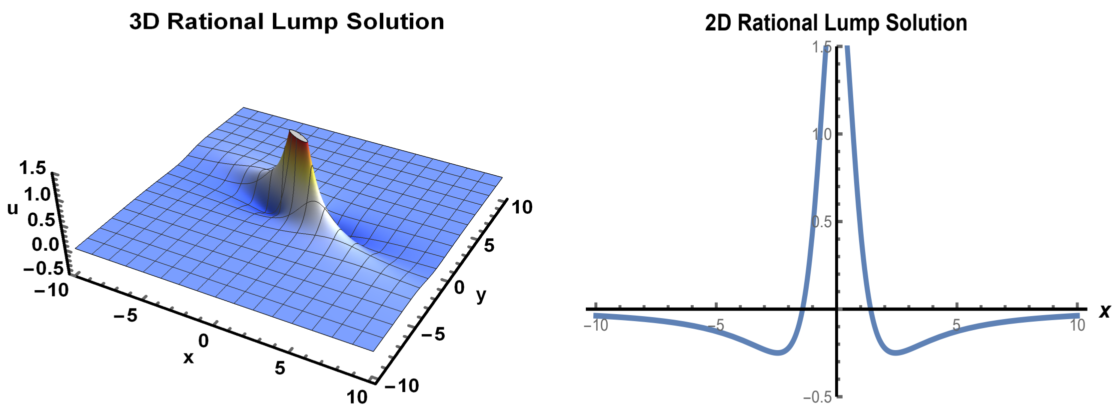

(a) 3D rational lump **(b)** 2D rational lump

Figure 9. Two and three-dimensional rational lump solution where $-10 \leq x,\ y \leq 10$.

Remark 4. *We identify several types of solutions in this article using a specific set of parameters and the modified Riccati sub-equation function method. Using different parameter sets or boundary conditions will help researchers find additional solution families.*

6. Results and discussion

The MRSEFM, applied here for the first time to Eq (1.1), produces closed-form solutions by driving the discriminant

$$\Delta = \beta^2 - 4\alpha\gamma$$

of the Riccati auxiliary equation through three regimes in a single unified calculation, an efficiency that single-branch methods such as the tanh-expansion or the exp-function method cannot match. The balance condition fixes $n = 2$, yielding the tractable coefficient set (3.7), from which all five travelling-wave families emerge. The discriminant Δ defined three solution branches within this family. The hyperbolic branch ($\Delta > 0$) with real elliptic modulus generates solutions $u_{1,1}$ and $u_{1,2}$: the bright soliton and singular soliton, respectively; the trigonometric branch ($\Delta < 0$) with pure imaginary modulus generates solutions $u_{2,1}$ and $u_{2,2}$: periodic wave trains of squared sinusoids; and the rational branch ($\Delta = 0$) gives solution $u_{3,1}$. The sech^2 ansatz generated a bell-shaped soliton with explicit amplitude formula

$$\Xi = -\frac{3(k^2\alpha_3 - l\omega\alpha_1 + m^2\alpha_4)}{kl\alpha_2}$$

and the Hirota method generated the non-singular rational lump solution U_{Lump}, which decays algebraically as $\mathscr{O}(\frac{1}{x^2})$.

On novelty and verification: The seven solution families listed above extend prior work by providing explicit closed-form expressions for all coefficients and parameters in terms of the original Eq (1.1). A comparison with the literature (Table 2) shows that the specific forms, parameter dependencies, and joint application of the MRSEFM with the sech^2 ansatz and Hirota method yield solutions not previously reported in combination for this model. However, we acknowledge that individual solution types (bright solitons, periodic waves, lumps) have appeared in prior studies of related equations. The present work systematizes these results and quantifies the role of the dispersion parameter α_4 in shaping solution property contribution not highlighted in the cited literature. All seven solutions have been substituted back into the reduced ODE (3.2) using symbolic algebra software.

Regarding the physical interpretation of complex-valued solutions: The solutions $u_{1,1}$, $u_{1,2}$, $u_{2,1}$, $u_{2,2}$, and $u_{3,1}$ contain complex expressions due to the Riccati parameters becoming complex. These represent envelope waves where the real part corresponds to the physical wave amplitude and the imaginary part represents phase modulation. In the context of nonlinear optics, such solutions describe pulse propagation with phase variations. In fluid dynamics, the imaginary component can represent secondary wave modes or modulation effects. For the standard wave interpretation, only the real-valued solutions (bell soliton and lump) are directly admissible as physical fields, while the complex solutions may require further physical interpretation depending on the specific application context.

Table 2. Comparison of our results with related work on the (3+1)-dimensional P-type and analogous equations.

Article	Studied model	Used method	Types of the obtained solutions	Present work and novelty
Dhiman & Kumar [24]	P-type (3+1)-D	Newly created methodology	Multi-peakons; lumps	New: five families by MRSEFM; closed-form bell soliton
Mohan et al. [13]	P-type (3+1)-D	Painlevé + Hirota	Higher-order rogue waves; dispersive solitons	New: sech^2, csch^2, tan, cot, rational branches; explicit a, b
Nadeem et al. [25]	P-type (3+1)-D	Modified Sardar sub-equation method	rational, hyperbolic, exponential, and trigonometric functions	New: MRSEFM trig./rational branches; distinct lump τ-function
Murad et al. [26]	Conformable fractional P-type	Kudryashov and Bernoulli equation methods	traveling wave solutions	Integer-order baseline; new: all MRSEFM & lump families
Ali et al. [27]	New conformable P-type (3+1)-D	Kumar-Malik and the new extended direct algebraic methods	The analytical solutions; numerical profiles	Non-fractional; New: more families via MRSEFM
Liu [28]	Painlevé-integrable fluid equation	Symbolic/direct	Soliton structures	Different equation; lump & bell soliton extend fluid-wave picture
Beenish et al. [29]	Extended (3+1)-D KP equation	Extended hyperbolic function and the generalized logistic equation methods	Lie symmetry analysis and derive lump, breather, and soliton solutions	P-type geometry; lump (5.12) structurally new
Singh & Ray [30]	Variable-coeff. pKP system	Painlevé + analytical	Diverse solutions; integrability proof	Constant-coeff. model; MRSEFM branches new
Senol & Erol [15]	Conformable P-type (3+1)-D	Analytical & numerical	Wave solutions	Different operator; MRSEFM not applied
Jawarneh et al. [23]	Gardner equation	Riccati-modified extended simple equation	Analytical wave solutions	Different equation; method variant
Present work	P-type (3+1)-D, Eq (1.1)	MRSEFM + sech^2 + Hirota	$u_{1,1}$, $u_{1,2}$, $u_{2,1}$, $u_{2,2}$, $u_{3,1}$, bell soliton, rational lump	Systematic treatment: unified MRSEFM framework; parameter dependencies; soliton formulas. The combined use of all three methods in one model is new.

Note: "New" indicates solution forms or method combinations not reported in that particular reference. The present work contributes a systematic application of MRSEFM to this model with explicit analysis of the role of dispersion parameter α_4, which had not been previously quantified.

The explicit amplitude formula makes it clear that the third spatial coordinate, scaled by coefficient α_4, directly affects soliton height and width: A quantitative measure not previously known for this equation. Physically, localized energy pulses were modeled by the bright soliton and bell soliton in shallow water, nonlinear optics, and Bose-Einstein condensates; periodic wave trains model the modulation of nonlinear wave fields in stratified fluids; and the rational lump effectively models the sudden onset of elevation that decays algebraically, characteristic of rogue waves in the ocean and coherent structures in plasma. These claimed applications are supported by the mathematical structure of the solutions: The bell soliton and bright soliton solutions are known to model localized energy pulses in shallow water and nonlinear optics; the periodic wave trains model modulation in stratified fluids; and the rational lump models algebraic decay patterns characteristic of rogue waves. However, these applications would benefit from further validation through numerical simulations and physical experiments, which we leave for future work.

7. Conclusions

In this manuscript, we employed the MRSEFM, direct sech^2 ansatz, and Hirota bilinear formalism to construct solutions of the generalized $(3+1)$-dimensional P-type nonlinear wave Eq (1.1). The PDE reduction

$$\xi = kx + ly + mz - \omega t,$$

with balance principle ($n = 2$) generated the unified coefficient set (3.7). The discriminant Δ defined three solution branches within this family. The hyperbolic branch ($\Delta > 0$) with real elliptic modulus generated solutions $u_{1,1}$ and $u_{1,2}$: the bright soliton and singular soliton, respectively; the trigonometric branch ($\Delta < 0$) with pure imaginary modulus generated solutions $u_{2,1}$ and $u_{2,2}$: periodic wave trains of squared sinusoidal; and the rational branch ($\Delta = 0$) gives solution $u_{3,1}$. The sech^2 ansatz generated a bell-shaped soliton with explicit amplitude formula

$$\Xi = -\frac{3(k^2\alpha_3 - l\omega\alpha_1 + m^2\alpha_4)}{kl\alpha_2},$$

and the Hirota method generated the non-singular rational lump solution U_{Lump}, which decays algebraically as $\mathcal{O}(\frac{1}{x^2})$. All seven solutions are consistent with the governing equation, and their forms depend explicitly on the original PDE parameters α_1–α_4.

A comparison with works (Table 2) demonstrates that while individual solution types (bright solitons, periodic waves, lumps) have appeared in prior studies of related equations, we provide a systematic treatment of the P-type equation using the MRSEFM with explicit parameter dependencies and a quantified role of the dispersion parameter α_4, which had not been previously highlighted. The combined application of all three methods to a single model is new, as is the explicit verification of all solutions through direct substitution.

The explicit amplitude formula makes it clear that the third spatial coordinate, scaled by coefficient α_4, directly affects soliton height and width: A quantitative measure not previously known for this equation. Physically, localized energy pulses were modeled by the bright soliton and bell soliton in shallow water, nonlinear optics, and Bose-Einstein condensates; periodic wave trains model the modulation of nonlinear wave fields in stratified fluids; and the rational lump effectively models the sudden onset of elevation that decays algebraically, characteristic of rogue waves in the ocean and coherent structures in plasma. We leave it to researchers to uncover multi-soliton and soliton-lump interactions through higher-order Hirota τ-functions, construct higher-order rational "rogue" waves from the rational seed solution $u_{3,1}$ through Darboux transformation, and extend the MRSEFM to apply to the conformally fractional generalization of Eq (1.1). Stability of the derived solutions under stochastic perturbation and a systematic conservation-law verification for each solution are also open questions of physical importance.

Author contributions

The authors investigated the research model, developed applications, and performed calculations. All authors contributed equally to the writing of the paper and equally to the assessment of the results. L. Zhan: investigation, methodology, resources, validation, formal analysis, visualization, writing original draft; A. A. Mahmud: conceptualization, supervision, writing original draft, software, writing-review & editing, methodology; H. M. Baskonus: supervision, conceptualization, methodology, investigation, formal analysis, visualization. All authors have read and approved the final version of the manuscript for publication.

Use of Generative-AI tools declaration

The authors declare they have not used artificial intelligence (AI) tools in the creation of this article.

Conflict of interest

The authors indicate that there are no conflicts of interest.

References

1. R. Hirota, *The Direct method in soliton theory*, Cambridge University Press, 2004. https://doi.org/10.1017/CBO9780511543043
2. A. M. Wazwaz, *Partial differential equations and solitary waves theory*, Springer, 2009. https://doi.org/10.1007/978-3-642-00251-9
3. N. J. Zabusky, M. D. Kruskal, Interaction of "solitons" in a collisionless plasma and the recurrence of initial states, *Phys. Rev. Lett.*, **15** (1965), 240–243. https://doi.org/10.1103/PhysRevLett.15.240
4. C. S. Gardner, J. M. Greene, M. D. Kruskal, R. M. Miura, Method for solving the Korteweg–de Vries equation, *Phys. Rev. Lett.*, **19** (1967), 1095–1097. https://doi.org/10.1103/PhysRevLett.19.1095
5. D. J. Korteweg, G. de Vries, On the change of form of long waves advancing in a rectangular canal, and on a new type of long stationary waves, *London Edinburgh Dublin Philos. Mag. J. Sci.*, **39** (1895), 422–443. https://doi.org/10.1080/14786449508620739
6. B. A. Malomed, Multidimensional soliton systems, *Adv. Phys. X*, **9** (2024), 2301592. https://doi.org/10.1080/23746149.2023.2301592
7. M. J. Ablowitz, P. A. Clarkson, *Solitons, nonlinear evolution equations and inverse scattering*, Cambridge University Press, 1991. https://doi.org/10.1017/CBO9780511623998
8. B. B. Kadomtsev, V. I. Petviashvili, On the stability of solitary waves in weakly dispersing media, *Sov. Phys. Dokl.*, **15** (1970), 539–541.

9. J. Weiss, M. Tabor, G. Carnevale, The Painlevé property for partial differential equations, *J. Math. Phys.*, **24** (1983), 522–526. https://doi.org/10.1063/1.525721
10. A. M. Wazwaz, Painlevé integrability and lump solutions for two extended (3+1)- and (2+1)-dimensional Kadomtsev–Petviashvili equations, *Nonlinear Dyn.*, **111** (2023), 3623–3632. https://doi.org/10.1007/s11071-022-08074-2
11. S. Kumar, B. Mohan, A direct symbolic computation of center-controlled rogue waves to a new Painlevé-integrable (3+1)-D generalized nonlinear evolution equation in plasmas, *Nonlinear Dyn.*, **111** (2023), 16395–16405. https://doi.org/10.1007/s11071-023-08683-5
12. N. Akhmediev, A. Ankiewicz, J. M. Soto-Crespo, Rogue waves and rational solutions of the nonlinear Schrödinger equation, *Phys. Rev. E*, **80** (2009), 026601. https://doi.org/10.1103/PhysRevE.80.026601
13. B. Mohan, S. Kumar, R. Kumar, Higher-order rogue waves and dispersive solitons of a novel P-type (3+1)-D evolution equation in soliton theory and nonlinear waves, *Nonlinear Dyn.*, **111** (2023), 20275–20288. https://doi.org/10.1007/s11071-023-08938-1
14. T. Wang, L. Tian, Z. Ma, Z. Yang, H. Han, Bifurcation soliton solutions, M-lump, breather waves, and interaction solutions for (3+1)-dimensional P-type equation, *Chaos Solitons Fract.*, **192** (2025), 115932. https://doi.org/10.1016/j.chaos.2024.115932
15. M. Şenol, M. Ö. Erol, New conformable P-type (3+1)-dimensional evolution equation and its analytical and numerical solutions, *J. New Theory*, **46** (2024), 71–88. https://doi.org/10.53570/jnt.1420224
16. K. A. Muhamad, On the traveling wave solutions to the complex nonlinear second-order modified unstable (1+1)-dimensional Schrödinger equation, *Int. J. Math. Comput. Eng.*, **3** (2025), 349–364. https://doi.org/10.2478/ijmce-2025-0025
17. A. A. Mahmud, K. A. Muhamad, T. Tanriverdi, Further characteristics for certain newly formed solutions for two significant mathematical models by utilization of an efficient semi-analytic method, *Int. J. Math. Comput. Eng.*, **4** (2026), 419–438. https://doi.org/10.2478/ijmce-2026-0022
18. A. A. Mahmud, K. A. Muhamad, T. Tanriverdi, H. M. Baskonus, Analyzing soliton dynamics of the solutions of (3+1)-dimensional Gardner–Kadomtsev–Petviashvili model for pulse propagation in single-mode optical fibers, *Z. Angew. Math. Phys.*, **77** (2026), 141. https://doi.org/10.1007/s00033-026-02766-0
19. A. M. Sultan, D. Lu, M. Arshad, H. U. Rehman, M. S. Saleem, Soliton solutions of higher order dispersive cubic-quintic nonlinear Schrödinger equation and its applications, *Chin. J. Phys.*, **67** (2020), 405–413. https://doi.org/10.1016/j.cjph.2019.10.003
20. A. A. Mahmud, Considerable traveling wave solutions of the generalized Hietarinta-type equation, *Int. J. Math. Comput. Eng.*, **3** (2025), 185–200. https://doi.org/10.2478/ijmce-2025-0015
21. A. A. Mahmud, K. A. Muhamad, T. Tanriverdi, Dynamical behavior and soliton solutions of the (2+1)-dimensional Novikov–Veselov system of equations, *Nonlinear Anal. Comput. Simul.*, **1** (2026), 1. https://doi.org/10.53941/nacs.2026.100001
22. J. Muhammad, U. Younas, Dynamics of new truncated M-fractional derivative wave structures to the nonlinear Zhiber-Shabat equation arising in variety of fields, *Int. J. Math. Comput. Eng.*, **4** (2026), 145–160. https://doi.org/10.2478/ijmce-2026-0009

23. Y. Jawarneh, M. Y. Almusawa, I. Haleemzai, A. H. Hakami, A. A. H. Ahmadini, A. Albaity, New analytical wave solutions for the Gardner equation via the Riccati-modified extended simple equation method, *Sci. Rep.*, **16** (2026), 18088. https://doi.org/10.1038/s41598-026-46592-w
24. S. K. Dhiman, S. Kumar, Analyzing specific waves and various dynamics of multi-peakons in (3+1)-dimensional P-type equation using a newly created methodology, *Nonlinear Dyn.*, **112** (2024), 10277–10290. https://doi.org/10.1007/s11071-024-09588-7
25. M. Nadeem, O. A. Arqub, A. H. Ali, H. A. Neamah, Bifurcation, chaotic analysis and soliton solutions to the (3+1)-dimensional P-type model, *Alexandria Eng. J.*, **107** (2024), 245–253. https://doi.org/10.1016/j.aej.2024.07.032
26. M. A. S. Murad, U. Younas, E. Hussain, F. S. Alshammari, Analysis of soliton profiles of the generalized P-type equation with conformable derivative via two distinct approaches, *Fractals*, **34** (2026), 2650054. https://doi.org/10.1142/S0218348X26500544
27. M. Ali, M. B. Riaz, N. Ahmed, M. Z. Baber, A. Akgül, Dynamical wave structures for time-fractional (3+1)-dimensional P-type model via two improved techniques, *Partial Differ. Equations Appl. Math.*, **16** (2025), 101303. https://doi.org/10.1016/j.padiff.2025.101303
28. J. G. Liu, Soliton structures for the (3+1)-dimensional Painlevé integrable equation in fluid mediums, *Sci. Rep.*, **14** (2024), 11581. https://doi.org/10.1038/s41598-024-62314-6
29. Beenish, M. Samreen, F. S. Alshammari, Exploring solitary wave solutions of the generalized integrable Kadomtsev-Petviashvili equation via Lie symmetry and Hirota's bilinear method, *Symmetry*, **17** (2025), 710. https://doi.org/10.3390/sym17050710
30. S. Singh, S. S. Ray, The Painlevé integrability and abundant analytical solutions for the potential Kadomtsev–Petviashvili (pKP) type coupled system with variable coefficients arising in nonlinear physics, *Chaos Solitons Fract.*, **175** (2023), 113947. https://doi.org/10.1016/j.chaos.2023.113947